

Supporting Information

An electrochemical resistor for discharging spent lithium-ion batteries:

Discharging mechanism and environmental impact analysis

Xin Qu^{1,3}, Fangzhao Pang^{1,3}, Shiyu Wang¹, Xiang Chen^{1,3*}, Xinyu Li^{1,2}, Fengyin Zhou^{1,3}, Danfeng Wang^{1,2}, Shuaibo Gao^{1,2,3}, Dihua Wang^{1,2,3,4}, Huayi Yin^{1,2,3,4*}

1. School of Resource and Environmental Science, Wuhan University, 299 Bayi Road, Wuchang District, Wuhan 430072, P. R. China.
2. Hubei International Scientific and Technological Cooperation Base of Sustainable Resource and Energy, Wuhan University, Wuhan 430072, China
3. Hubei Provincial Key Laboratory of Biomass Resource Chemistry and Environmental Biotechnology
4. Joint Center of Green Manufacturing of Energy Storage Materials of Wuhan University and Chilwee, Wuhan 430072, P. R. China

corresponding author: Xiang Chen, chenxiang35930@whu.edu.cn

Huayi Yin, yinhuayi@whu.edu.cn

This file includes:

Figures S1 to S21

Table S1 to S8

Life cycle assessment (LCA)

There are four discharge models (A, B, C, and D). A is ECR discharge with ferrocyanide (III/II), B is ECR discharge without ferrocyanide (III/II), C is Physical discharge, and D is Chemical discharge. Four discharge models can be specifically divided into seven discharge process, ferrocyanide (III/II)/Na₂SO₄ solution (A1), ferrocyanide (III/II)/NaCl solution (A2), Na₂SO₄/wire without ferrocyanide (III/II) (B1), NaCl/wire without ferrocyanide (III/II) (B2), physical resistor (C), Na₂SO₄ solution chemical discharge (D1), and NaCl solution chemical discharge (D2) (**Tab. S3**). In this study, LCA studies were conducted for the seven discharge processes to evaluate the differences in environmental impacts. The analysis followed ISO14040 and 14044 series, and was performed using SimaPro software¹.

In this work, LCA was developed to treat one thousand LIBs (functional units). The system boundary includes the inputs (energy and materials) and outputs (wastewater, exhaust gas, and waste) of the LIB discharge process, the production and maintenance of the discharge equipment were ignored. The life cycle inventory (LCI) of the LFP and NCM discharge processes is shown in **Tabs. S4-S5**. The upstream background data of energy and materials were obtained from the Ecoinvent 3.5 database representing the Chinese (CN) market^{2, 3}. When data representing the CN region were missing, global average (GLO) or rest of world (ROW) production data were used as substitutes. **Tabs. S7-S8** shows the list of background data for materials and energy selected for this study.

The total power of LFP and NCM considered in this study is 5.94 Wh and 12.81 Wh, respectively. 0.1 M K₄[Fe(CN)₆]/K₃[Fe(CN)₆] is selected as the comparison object for A1 and A2 processes. All salt concentration of A1, A2, B1, B2, D1, and D2 processes is 1 M. In the case of LFP treatment, the discharge efficiency of A1, A2, B1, and B2 processes is 98.3%, 94.9%, 16.56%, and 90.62%, respectively (**Tab. S1, Fig. S11**). In the case of NCM treatment, the discharge efficiency of A1, A2, B1, and B2 processes is 98.4%, 97.5%, 47.63%, and 82.81%, respectively (**Tab. S1, Fig. S11**). Due

to the preferable competitive reaction of the ferrocyanide (III/II) cycle with water splitting and the decomposition of NaCl, no obvious bubble generation was observed in A1 and A2 processes. Therefore, the energy loss of the water/NaCl decomposition process was ignored. Partial of the electrical energy released during the discharge process of B1 and B2 will decompose water or salt. It is assumed that 25% and 15% of the electrical energy released by B1 and B2 processes are used for water electrolysis. 15% of the electricity released by the B2 process is used for the electrolysis of NaCl. In this study, the A1, A2, B1, and B2 processes can recover the electricity released by LIB as heat energy. The heat recovery efficiency is assumed to be 80%. The system expansion method is considered to be the preferred method for treating byproducts in the system.³ In this study, the heat recovered in this work is treated by the system expansion method to avoid distribution. The C process uses a 2 Ω resistor to discharge batteries. It is assumed that the resistor is allowed to work within 500°C. The energy consumption for heat dissipation of the resistor is calculated as shown in **Eqs. S1-S2**. In this study, we assume the volume of a single battery is 16.53 ml, and the utilization rate of the water pool used for soaking batteries in the D1 and D2 processes is 10%. Considering the different levels of pollution discharged during the discharge process of the D1 and D2 processes (**Tab. S2**), the salt solutions used for soaking discharge in D1/LFP, D1/NCM, D2/LFP, and D2/NCM were replaced after treating 4, 4, 2, and 1 batches of LIBs (1 batch is 1000 18650-type LFP/NCM LIBs), respectively.

This study uses the ReCiPe 2016 method to assess the environmental impacts of discharge processes, including midpoint and endpoint environmental impact categories. The midpoint environmental impact categories include global warming potential (GWP), stratospheric ozone depletion (ODP), ionizing radiation (IRP), ozone formation, human health (OFHH), fine particulate matter formation (PMFP), ozone formation, terrestrial ecosystems (OFTE), terrestrial acidification (TAP), freshwater eutrophication (FEP), marine eutrophication (MEP), terrestrial ecotoxicity (TEP), freshwater ecotoxicity (FETP), marine ecotoxicity (METP), human carcinogenic

toxicity (HTPc), human noncarcinogenic toxicity (HTPcn), land use potential (LUP), mineral resource scarcity (SOP), fossil resource scarcity (FFP), and water consumption (WCP) (**Tab. S6**). The endpoint environmental impact categories include human health, ecosystems, and resources. The environmental impact assessment results of all discharge processes are shown in **Figs. S18-19**. In addition, this study uses sensitivity analysis to evaluate the environmental impact assessment results under different heat recovery performance (**Fig. S20**). When the heat recovery efficiency is 0%, the heat recovery of the discharge process is not considered. When the heat recovery efficiency is 100%, it means that all energy except the energy consumption of the side reaction is recovered.

Life cycle cost (LCC) uses the same system boundary and functional unit as LCA. The life cycle costs considered in this study include environmental and economic costs. The environmental prices of the midpoint environmental impact category are from the Environmental Prices Handbook (**Tab. S8**)⁴. Emissions and avoided pollution in the discharge process are considered as environmental costs and environmental benefits, respectively. In this study, the prices of sodium sulfate, sodium chloride, water and energy are 0.6 CNY/kg, 0.5 CNY/kg, 4 CNY/t and 1 CNY/kWh, respectively. The D1 and D2 processes are simpler to operate than other processes. Therefore, in the D1 and D2 scenarios, this study assumes that one worker can process 10,000 LIBs per day. In scenarios A1, A2, B1, B2, and C, it is assumed that one worker can process 5,000 LIBs per day. The labor cost of the worker is 200 CNY/d. The environmental cost analysis and total cost analysis of all discharge processes are shown in **Fig. S21** and **Fig. 6F**.

$$N = K \times P \times Q \times (3600 \times A \times B \times 1000) \quad (\text{S1})$$

$$Q = 1.8 \times \frac{F}{\Delta T \times 35.3} \quad (\text{S2})$$

N (W) is Heat dissipation power of the fan, K is 1.2, P is Atmospheric pressure (Pa), A (0.85) and B (0.7) is mechanical efficiency and wind conversion efficiency, respectively. F (W) is heat generation power when battery is discharging. ΔT (°C) is maximum operating temperature of resistance wire.

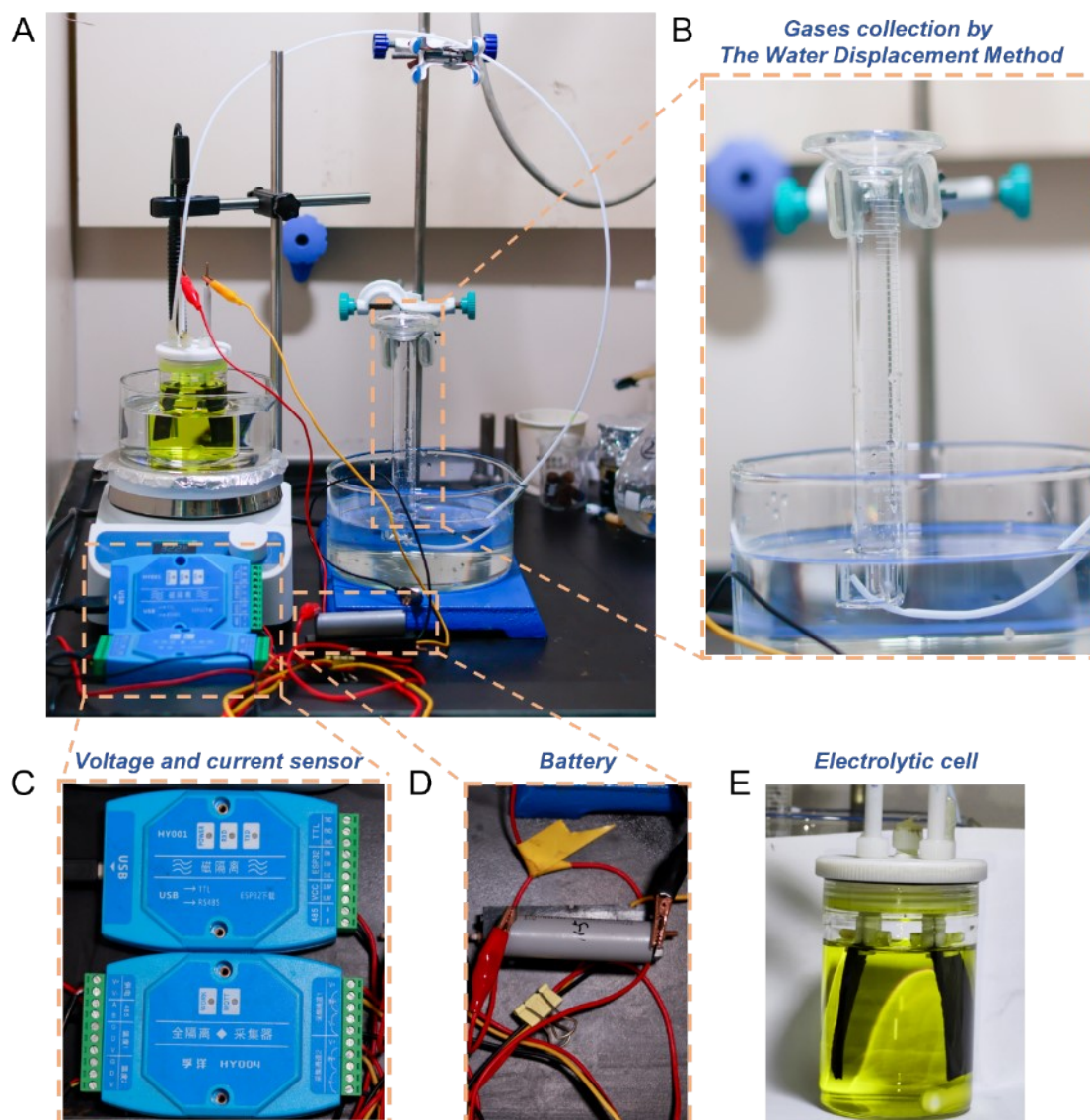


Fig. S1. Digital photos of Discharge device by ECR (A) Digital photos of an electrochemical resistor (ECR) assisted discharge device for LFP and NCM batteries in $[\text{Fe}(\text{CN})_6]^{4-}/[\text{Fe}(\text{CN})_6]^{3-}$ solution with $1\text{M Na}_2\text{SO}_4$ as the supporting electrolyte. (B) Gas collection device. (C) Current and voltage sensor. (D) A typical 18650-type LIB. (E) A typical ECR.

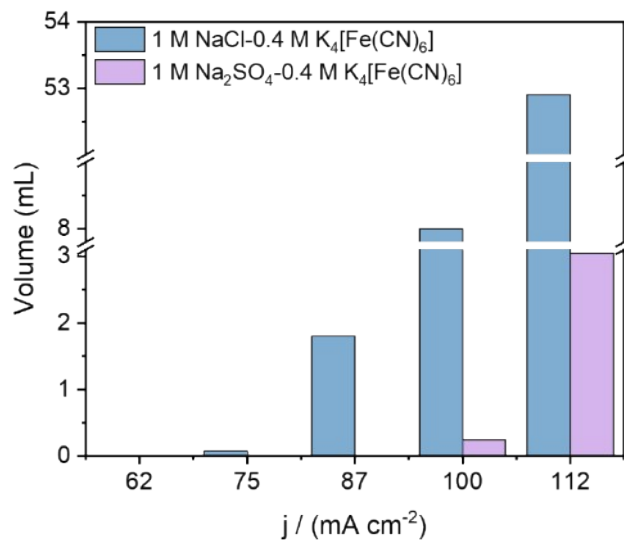


Fig. S2. Volumes of collected gases measured by the water displacement method operating at simulated constant current densities in 1 M NaCl and Na₂SO₄ supporting electrolyte, respectively (0.4 M K₄[Fe(CN)₆], 400 rpm, 30 °C).

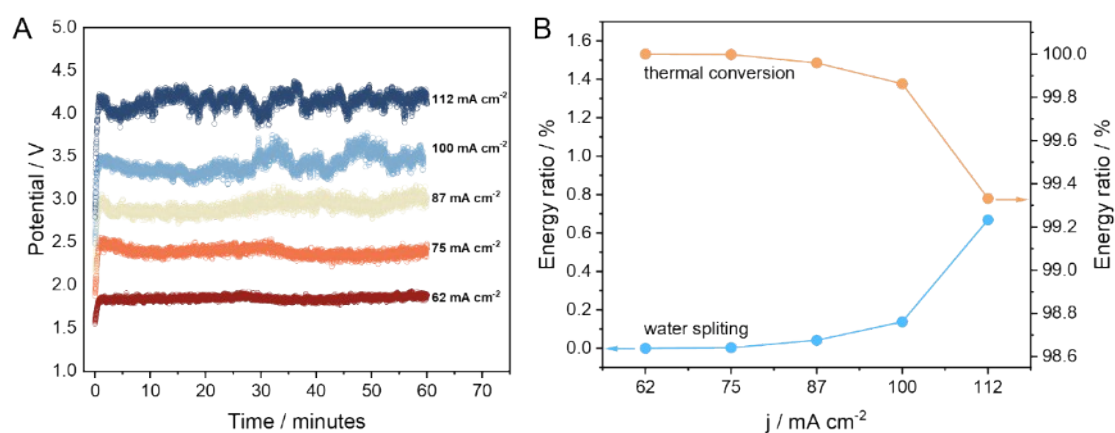


Fig. S3. Simulation of constant current discharge for carbon felt electrodes in 0.4 M $K_4[Fe(CN)_6]$ under different current densities (400 rpm, 30 °C, 1 M NaCl supporting electrolyte). (A) Voltage curves as a function of time, and the stabilized average voltages (1.84 V, 62 mA cm⁻²), (2.38 V, 75 mA cm⁻²), (2.91 V, 87 mA cm⁻²), (3.41 V, 100 mA cm⁻²), and (4.13 V, 112 mA cm⁻²). (B) Water splitting conversion efficiency E_C and thermal energy conversion efficiency E_T at different current densities.

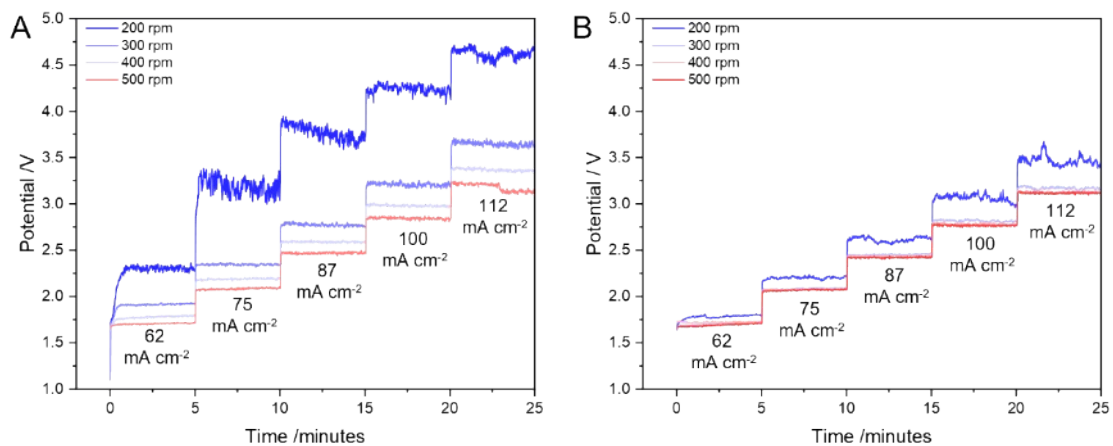


Fig. S4. Cell voltage changes with time under different current densities at different magnetic stirring speeds from 200 rpm to 500 rpm at 30 °C (0.4 M [Fe(CN)₆]⁴⁻/ [Fe(CN)₆]³⁻) in **(A)** 1 M NaCl supporting electrolyte and **(B)** 1 M Na₂SO₄ supporting electrolyte.

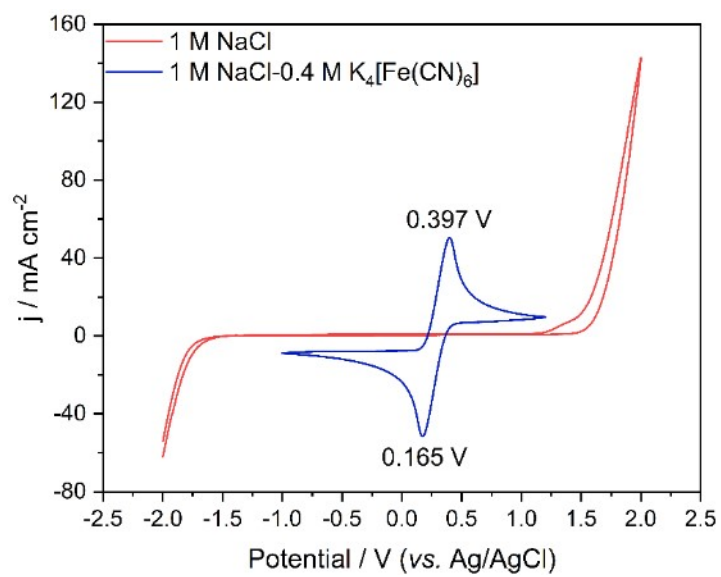


Fig. S5. Cyclic voltammograms (CV) of a glass carbon electrode in 1 M NaCl supporting electrolyte with and without 0.4 M $\text{K}_4[\text{Fe}(\text{CN})_6]$ (scan rate: 100 mV s^{-1}).

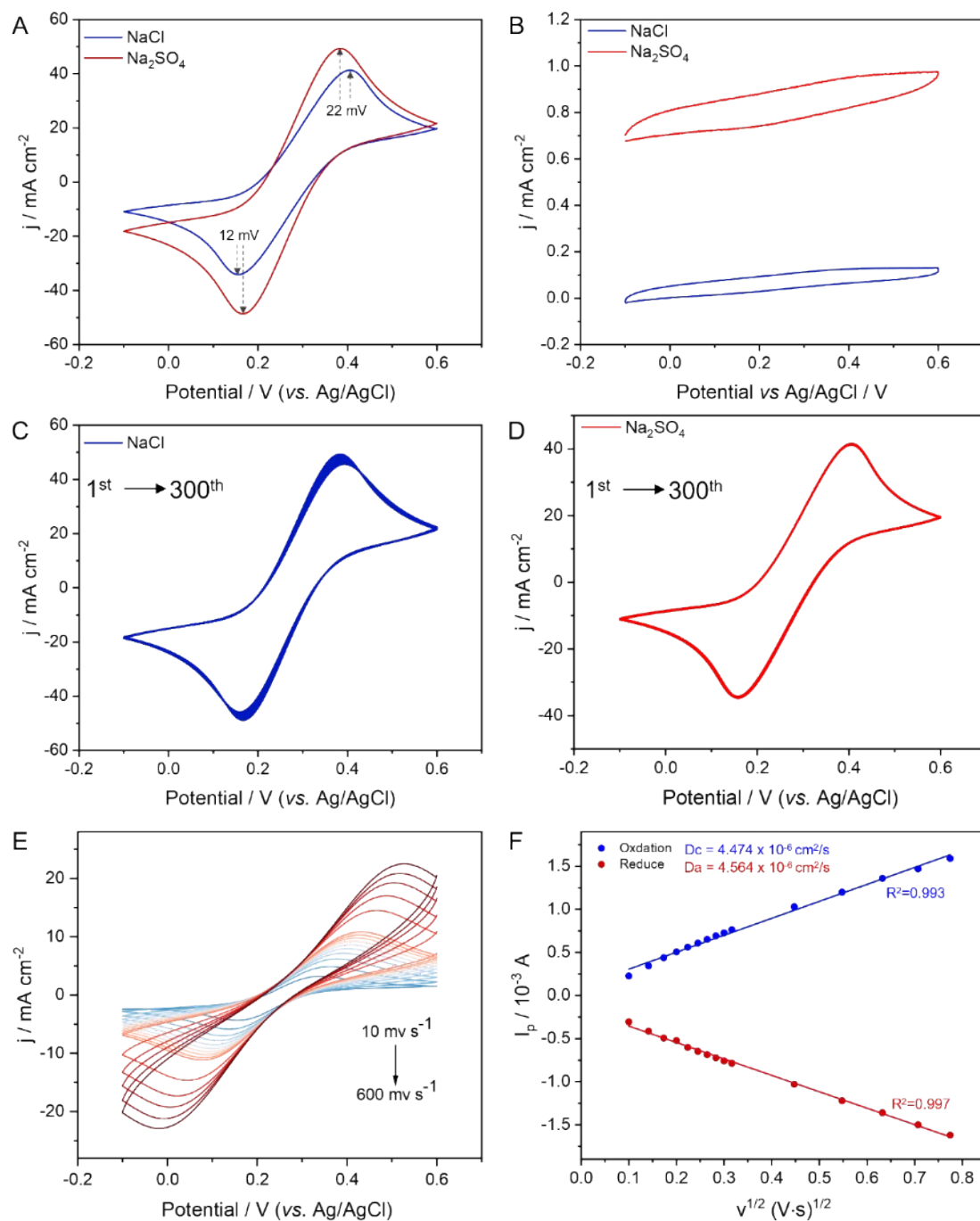


Fig. S6. Cyclic voltammograms (CVs) of a glass carbon electrode in 1 M NaCl/Na₂SO₄ supporting electrolyte (100 mV s⁻¹). (A) CVs recorded in 1 M NaCl/Na₂SO₄ solution containing 0.4 M K₄[Fe(CN)₆]. (B) CVs recorded in 1 M NaCl/Na₂SO₄ supporting electrolyte. (C) CVs recorded from 1st to 300th of cyclic voltammetry test in 1 M NaCl solution containing 0.4 M K₄[Fe(CN)₆]. (D) CVs recorded from 1st to 300th of cyclic voltammetry test in 1 M Na₂SO₄ solution containing 0.4 M K₄[Fe(CN)₆]. Electrochemical behaviors of K₄[Fe(CN)₆] in 1 M NaCl

under different scan rate from 10 mV S^{-1} to 600 mV S^{-1} . (E) CVs of $0.4 \text{ M K}_4[\text{Fe}(\text{CN})_6]$ in 1 M NaCl supporting electrolyte. (F) Diffusion coefficient (D_a/D_c) as a function of as a function of square root of scan rate ($v^{1/2}$) in 1 M NaCl .

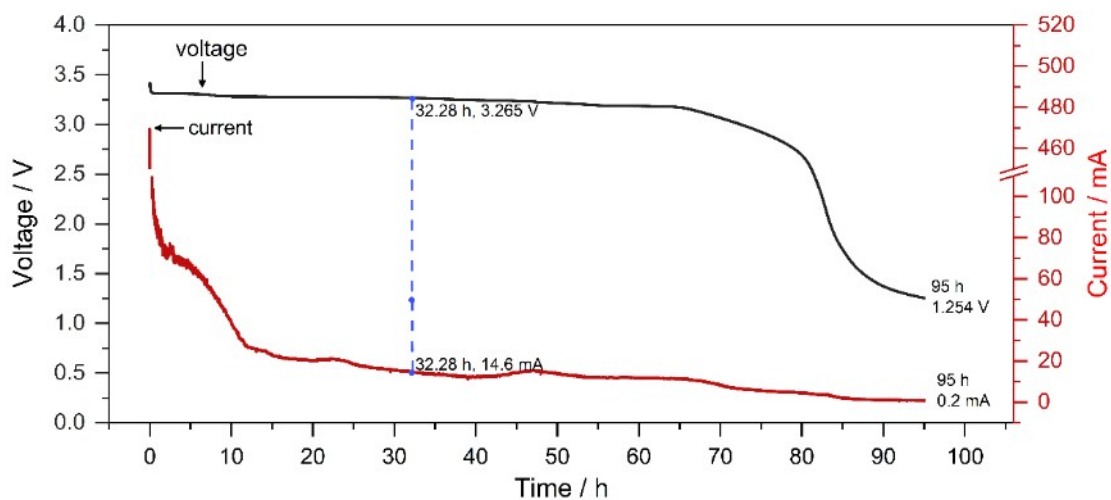


Fig. S7. Discharge voltage and current profiles of an LFP battery as a function of discharge time in 1 M NaCl solution (without adding $[\text{Fe}(\text{CN})_6]^{4-}/[\text{Fe}(\text{CN})_6]^{3-}$).

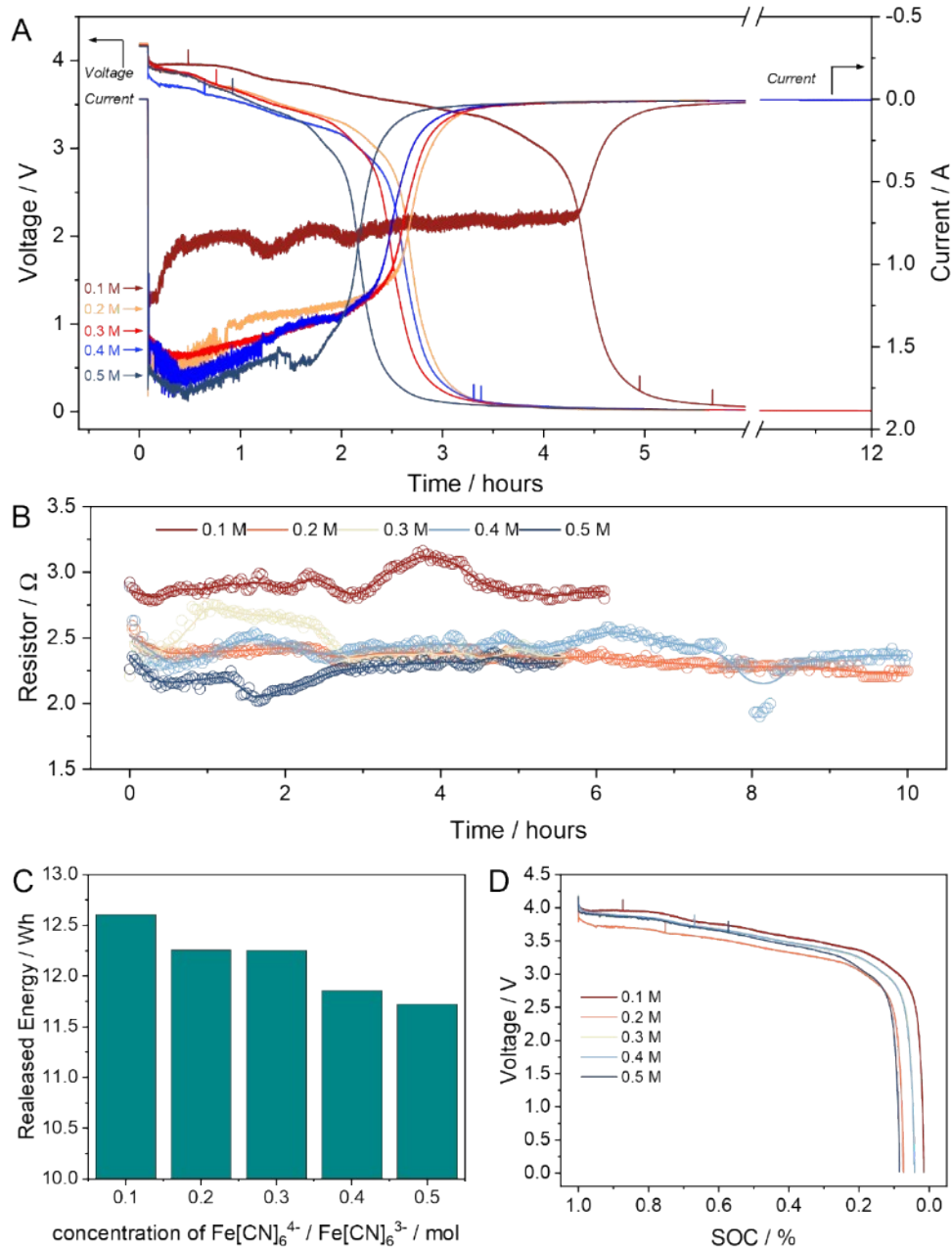


Fig. S8. Discharge performance of NCM batteries by the ECR method in different concentration of $K_4[Fe(CN)_6]/K_3[Fe(CN)_6]$ solution (0.1, 0.2, 0.3, 0.4, and 0.5 M) in 1 M Na_2SO_4 supporting electrolyte. (A) Voltage and current profile as a function of discharge time. (B) Dynamic resistance value (R_1) of different concentration of $K_4[Fe(CN)_6]/K_3[Fe(CN)_6]$ solution as a function of discharge time. (C) The total released electricity energy of NCM batteries (W_B) under different concentration of $K_4[Fe(CN)_6]/K_3[Fe(CN)_6]$ solution. (D) Battery voltage of NCM as a function of SOC state for different concentration of $K_4[Fe(CN)_6]/K_3[Fe(CN)_6]$

solution.

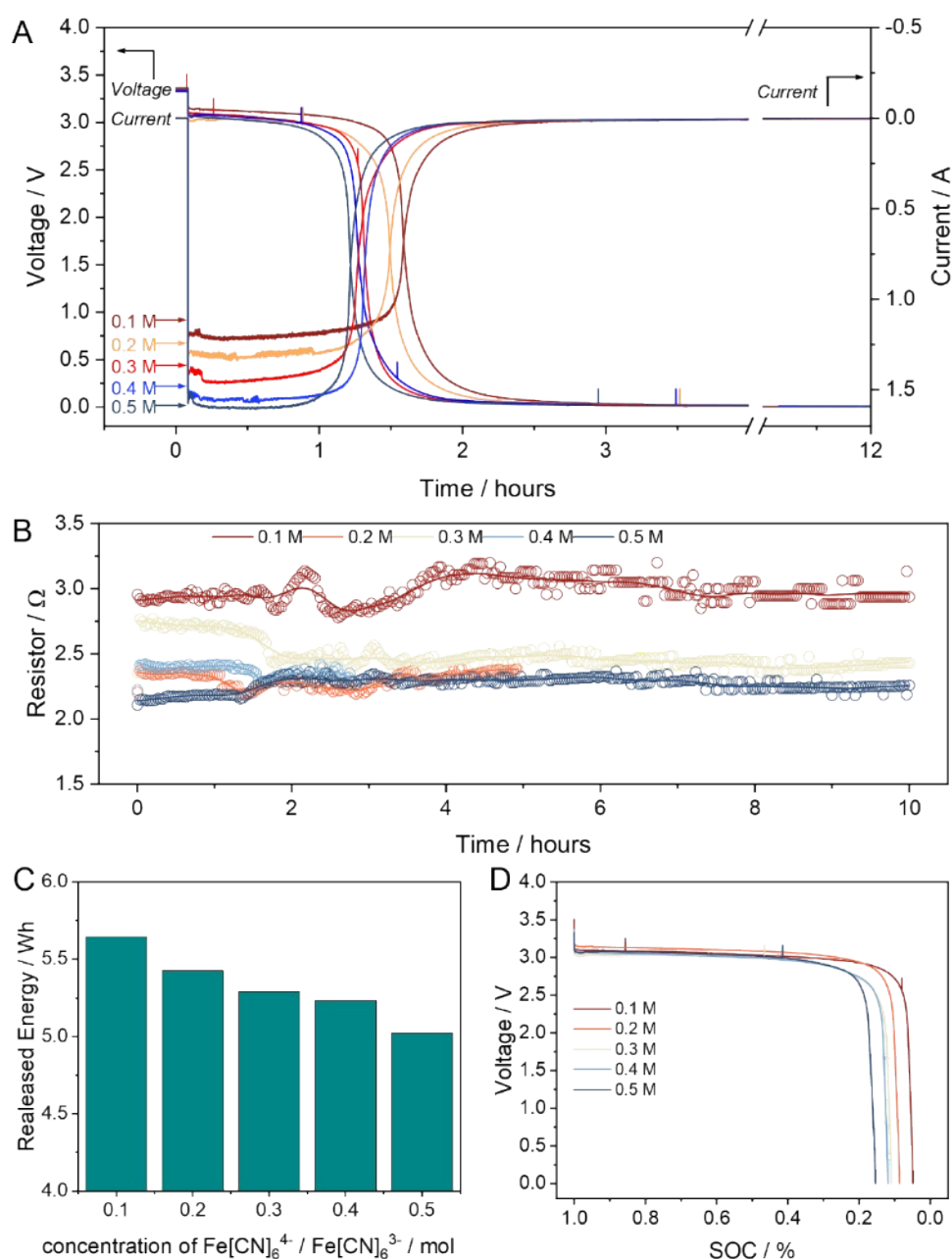


Fig. S9. Discharge performance of LFP batteries by the ECR method in different concentration of $K_4[Fe(CN)_6]/K_3[Fe(CN)_6]$ solution (0.1, 0.2, 0.3, 0.4, and 0.5 M) in 1 M NaCl supporting electrolyte. (A) Voltage and current profile as a function of discharge time. (B) Dynamic resistance value (R_1) of different concentration of $K_4[Fe(CN)_6]/K_3[Fe(CN)_6]$ solution as a function of discharge time. (C) The total released electricity energy of NCM batteries (W_B) under different concentration of $K_4[Fe(CN)_6]/K_3[Fe(CN)_6]$ solution. (D) Battery voltage of an LFP battery as a

function of SOC state for different concentration of $K_4[Fe(CN)_6]/K_3[Fe(CN)_6]$ solution.

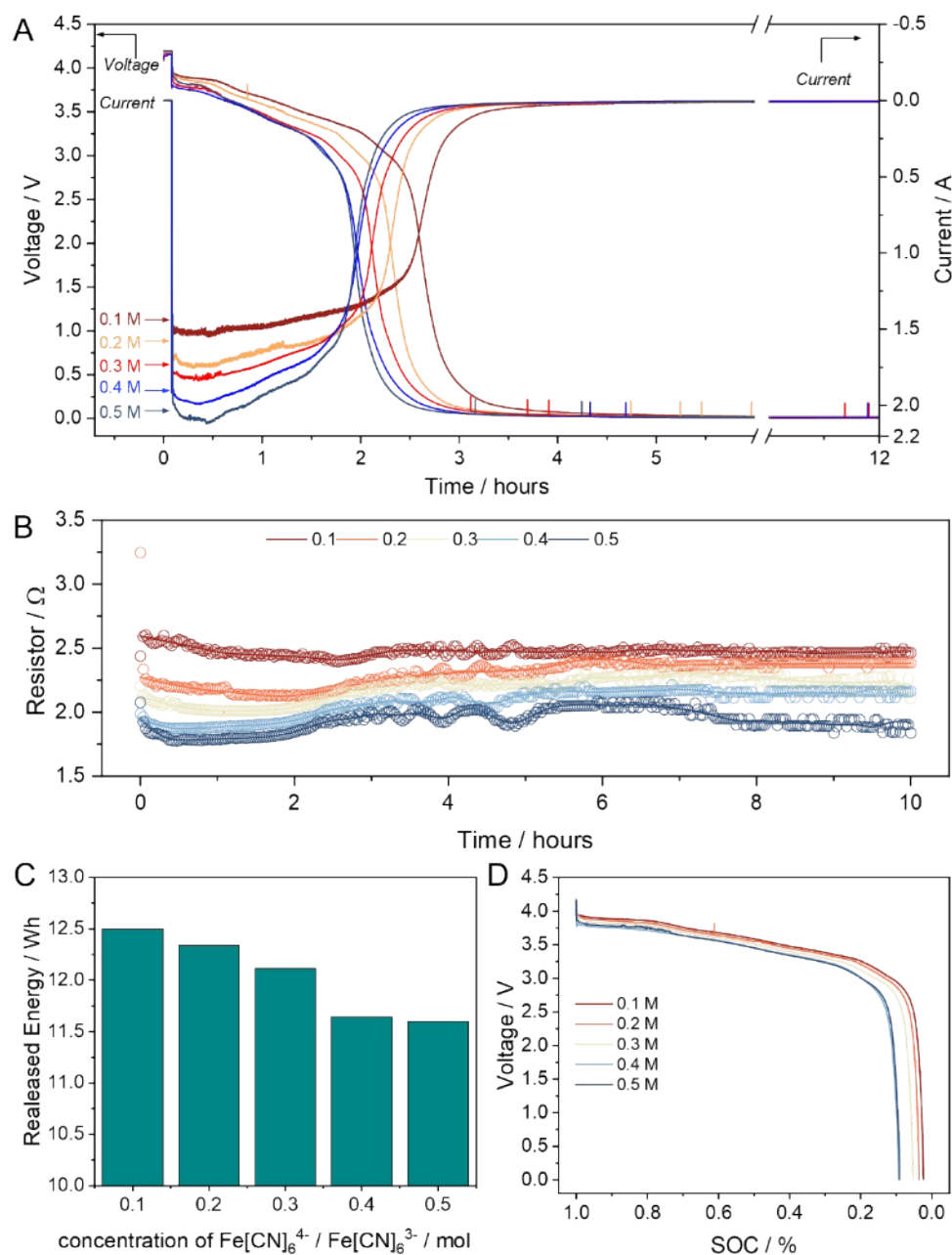


Fig. S10. Discharge performance of NCM batteries by the ECR method in different concentration of $K_4[Fe(CN)_6]/K_3[Fe(CN)_6]$ solution (0.1, 0.2, 0.3, 0.4, and 0.5 M) in 1 M NaCl supporting electrolyte. (A) Voltage and current profile as a function of discharge time. (B) Dynamic resistance value (R_1) of different concentration of $K_4[Fe(CN)_6]/K_3[Fe(CN)_6]$ solution as a function of discharge time. (C) The total released electricity energy of NCM batteries (W_B) under different

concentration of $K_4[Fe(CN)_6]/K_3[Fe(CN)_6]$ solution. **(D)** Battery voltage of a NCM battery as a function of SOC state for different concentration of the $K_4[Fe(CN)_6]/K_3[Fe(CN)_6]$ solution.

Tab. S1. Discharge time and the total released electric energy of LFP and NCM batteries in 0.1-0.5 M $K_4[Fe(CN)_6]/K_3[Fe(CN)_6]$ solution with Na_2SO_4 ($NaCl$) supporting electrolyte, and the dynamic resistance of the solution during the electrolysis.

	$K_4[Fe(CN)_6]$ / $K_3[Fe(CN)_6]$ (M)	LFP NaCl	LFP Na_2SO_4	NCM NaCl	NCM Na_2SO_4
Discharging time (minutes)	0.1	146.9	135.5	219.4	219.6
	0.2	130.7	123.6	211.2	188.1
	0.3	126.5	109.8	208.1	180.1
	0.4	126.1	106.1	205.1	168.5
	0.5	115.5	101.5	188.1	159.6
Released energy (Wh) and the ratio (%)	0.1	5.64, 94.9%	5.84, 98.3%	12.49, 97.5%	12.61, 98.4%
	0.2	5.42, 91.2%	5.73, 96.4%	12.34, 96.3%	12.25, 95.6%
	0.3	5.29, 89.1%	5.57, 93.7%	12.11, 94.5%	12.24, 95.5%
	0.4	5.23, 88.0%	5.45, 91.7%	11.64, 90.8%	11.85, 92.5%
	0.5	5.02, 84.5%	5.37, 90.4%	11.60, 90.5%	11.72, 91.4%
The resistance of solution (Ω)	0.1	2.98	2.78	2.91	2.47
	0.2	2.30	2.44	2.34	2.30
	0.3	2.48	2.24	2.47	2.19
	0.4	2.37	2.13	2.40	2.07
	0.5	2.26	1.99	2.36	1.93

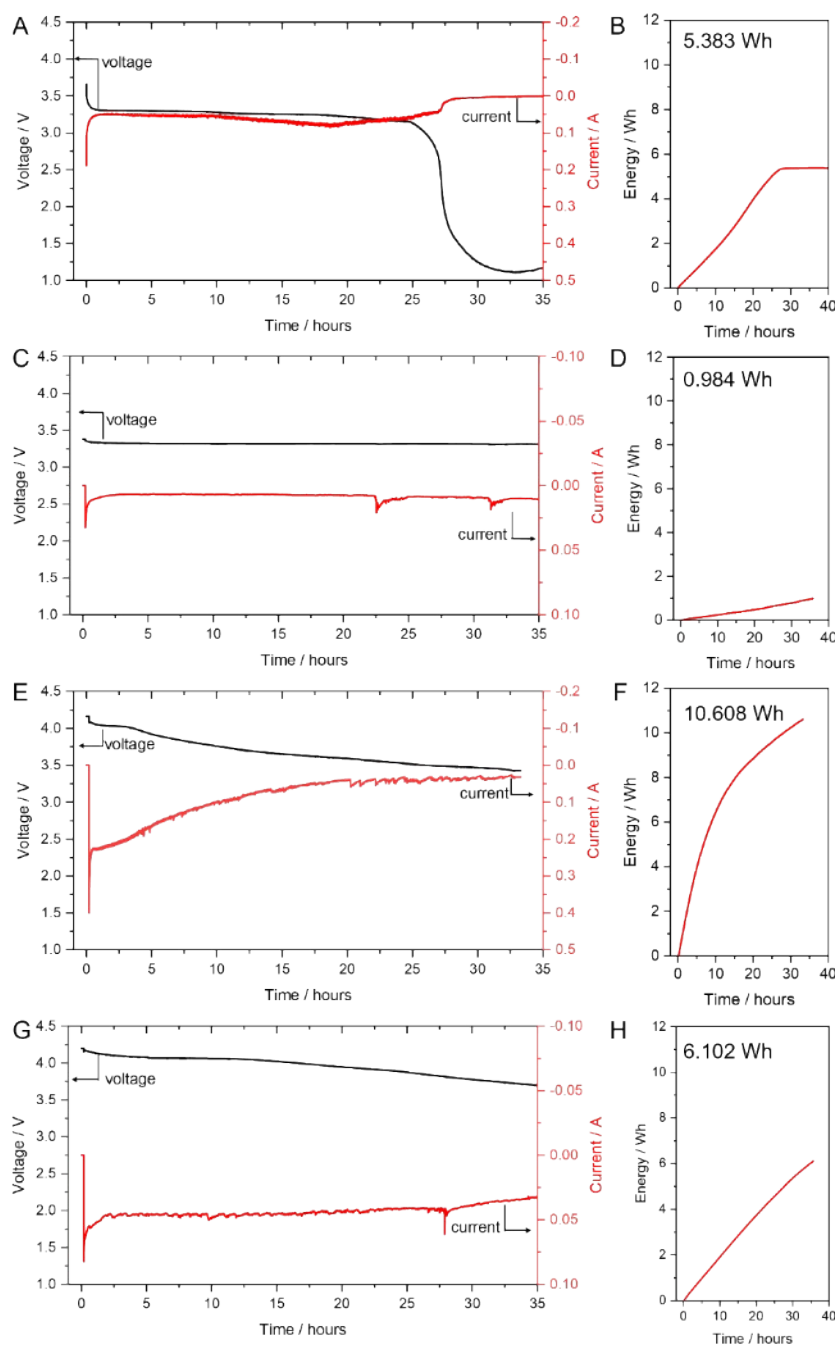
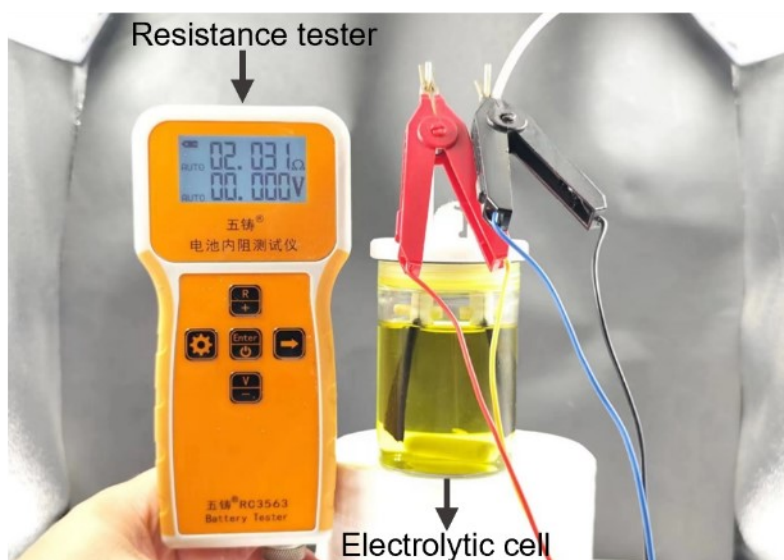


Fig. S11. Discharge performance of LFP batteries in 1 M NaCl/Na₂SO₄ supporting electrolyte solution without adding K₄[Fe(CN)₆]/K₃[Fe(CN)₆]. (A) Voltage and current profile as a function of a LFP battery in NaCl solution. **(B)** Released electric energy (5.94 Wh, 90.62% of discharge efficiency) of an LFP battery as a function of time in NaCl solution. **(C)** Voltage and current profile as a function of an LFP battery in Na₂SO₄ solution. **(D)** Released electric energy (0.984 Wh, 16.56% of discharge efficiency) of an LFP battery as a function of time in Na₂SO₄ solution.

The discharge of NCM batteries in 1 M NaCl/Na₂SO₄ supporting electrolyte solution without adding K₄[Fe(CN)₆]/K₃[Fe(CN)₆]. (E) Voltage and current profile as a function of a NCM battery in NaCl solution. (F) Released electric energy (10.608 Wh, 82.81% of discharge efficiency) of a NCM battery as a function of time in NaCl solution. (G) Voltage and current profile as a function of a NCM battery in Na₂SO₄ solution. (H) Released electric energy (6.102 Wh, 47.63% of discharge efficiency) of a NCM battery as a function of time in Na₂SO₄ solution.



Fig. S12. A standard physical resistor (2.031 Ω measured by a four-electrode resistance tester, RC3563, Wuzhu, China).



Static resistance of solution (Ω)	Concentration of $K_4[Fe(CN)_6]/K_3[Fe(CN)_6]$ (M)				
	0.1	0.2	0.3	0.4	0.5
1 M NaCl	2.66	2.34	2.16	2.13	2.02
1 M Na ₂ SO ₄	2.69	2.67	2.17	2.10	2.03

Fig. S13. Digital photos of and resistance tester and an ECR, and static resistance (R_2) of NaCl or Na₂SO₄ solution containing different concentrations of $K_4[Fe(CN)_6]/K_3[Fe(CN)_6]$ (model no.: RC3563, Wuzhu, China).

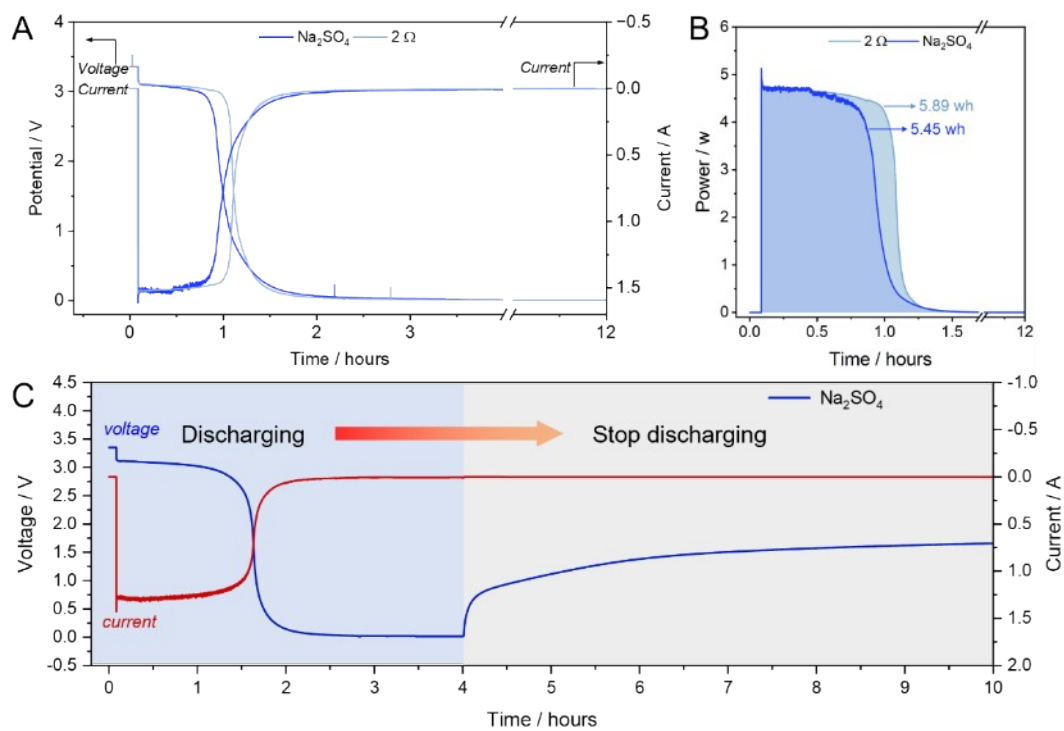


Fig. S14. Discharge performance of an LFP battery by an ECR containing 1 M Na_2SO_4 and 0.4 M $\text{K}_4[\text{Fe}(\text{CN})_6]/\text{K}_3[\text{Fe}(\text{CN})_6]$ and a 2Ω of physical resistor. (A) Voltage and current profiles as a function of time. (B) Discharge power profiles as a function of time during. (C) Voltage rebound profiles of a LFP battery.

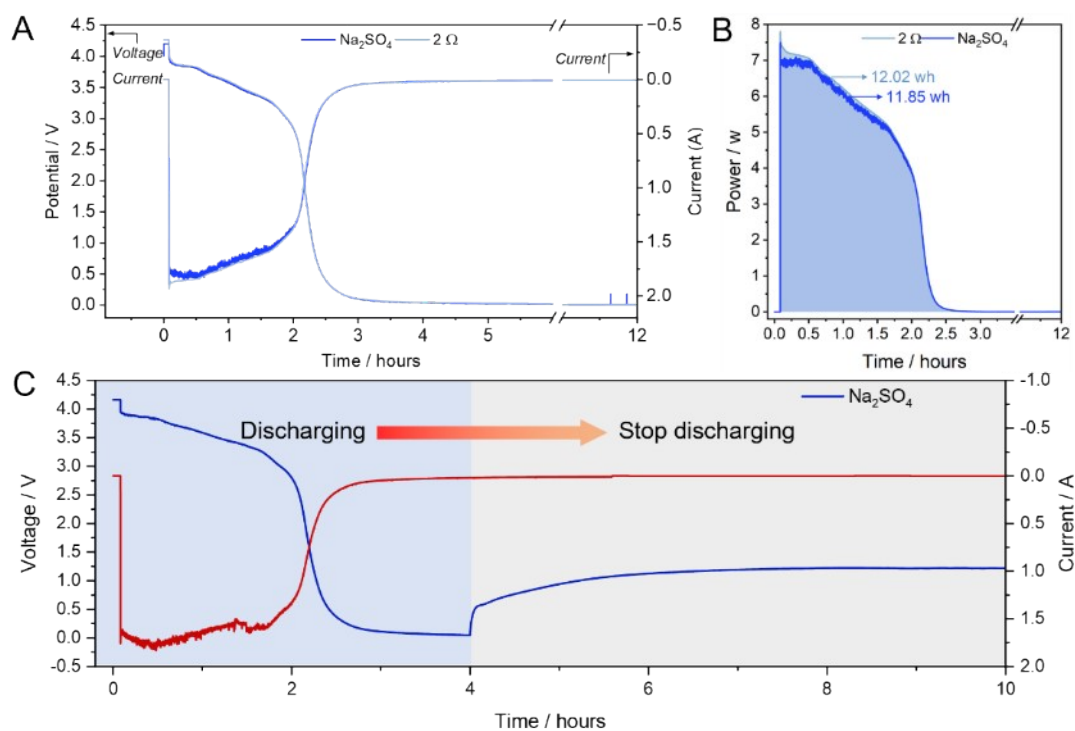


Fig. S15. The discharge performance of a NCM battery by an ECR containing 1 M Na_2SO_4 and 0.4 M $\text{K}_4[\text{Fe}(\text{CN})_6]/\text{K}_3[\text{Fe}(\text{CN})_6]$ and a 2Ω of physical resistor. (A) Voltage and current profiles as a function of time. (B) Discharge power profiles as a function of time during. (C) Voltage rebound profiles of a NCM battery.

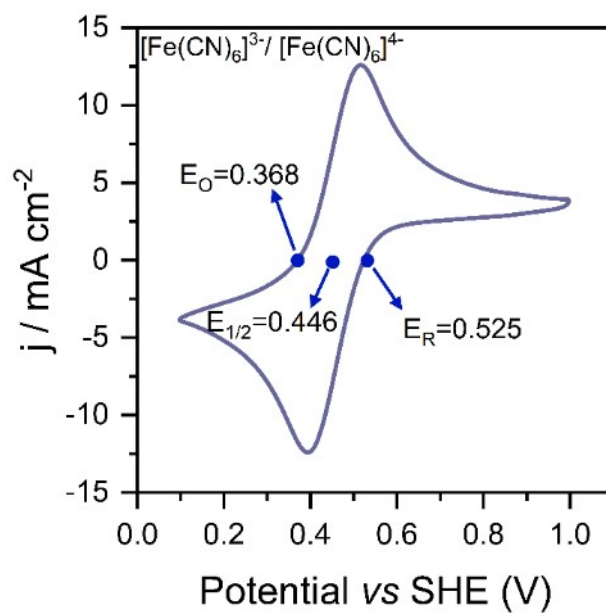


Fig. S16. Cyclic voltammogram (CV) test in 1 M Na_2SO_4 solution contains 0.4 M $[\text{Fe}(\text{CN})_6]^{4-}/[\text{Fe}(\text{CN})_6]^{3-}$ redox couple (100 mV s^{-1}), red and blue curves denote the reduction process of Fe(III) to Fe(II) and the oxidation process of Fe(II) to Fe(III), respectively.

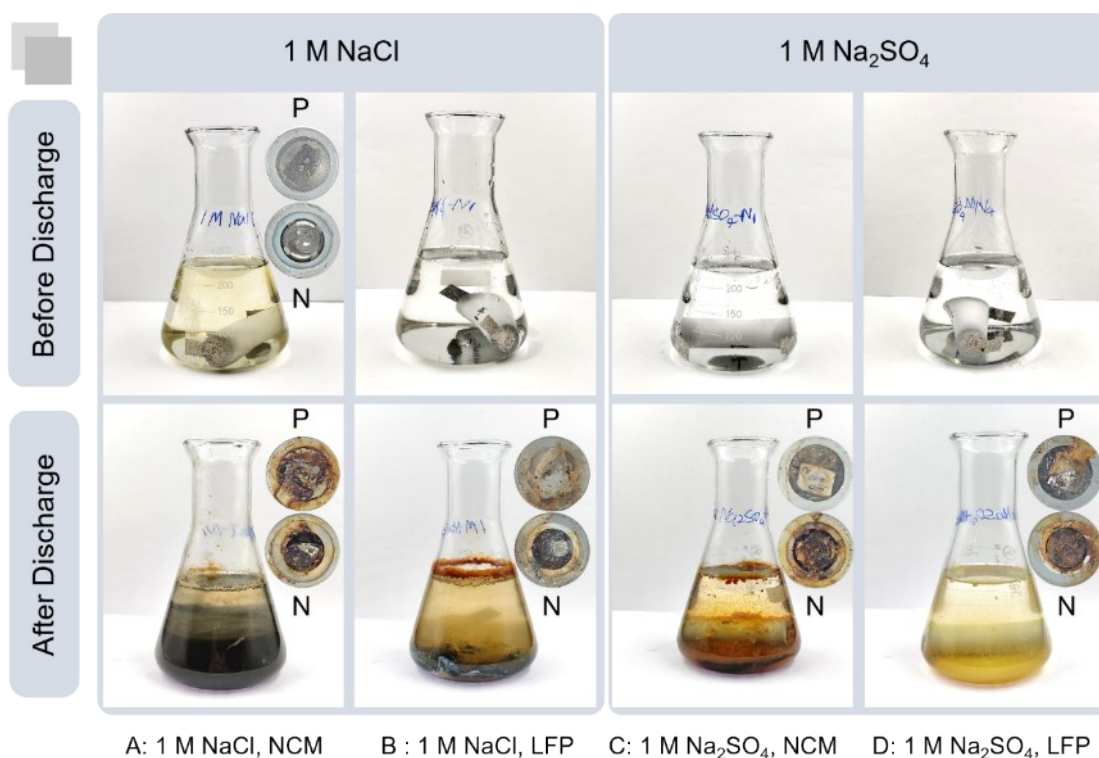


Fig. S17. The discharge performance of a NCM battery by an ECR containing 1 M Na₂SO₄ and 0.4 M K₄[Fe(CN)₆]/K₃[Fe(CN)₆] and a 2 Ω of physical resistor. (A) Voltage and current profiles as a function of time. (B) Discharge power profiles as a function of time during. (C) Voltage rebound profiles of a NCM battery. (P is the positive of battery and B is negative of battery)

Tab. S2 Pollution data of Li, Ni, Co, Mn, F, COD, and TOC for solution when LFP and NCM LIBs soaked in 1 M of NaCl/Na₂SO₄ solution after 24 hours.

	1 M NaCl		1 M Na ₂ SO ₄	
	NCM 622	LiFePO ₄	NCM 622	LiFePO ₄
Li / mg L ⁻¹	2.1	1.08	0.02	0.04
Ni / mg L ⁻¹	2.702	2.106	1.044	1.25
Co / mg L ⁻¹	1.381	1.361	0.831	0.841
Mn / mg L ⁻¹	0.904	0.405	0.173	0.205
Fe / mg L ⁻¹	61.73	1.343	1.193	0.623
F ⁻¹ / mg L ⁻¹	7.88	1.74	1.53	1.19
TOC / mg L ⁻¹	1270	468.4	85.94	83.88
COD / mg L ⁻¹	3530	2690	1350	1220

Tab. S3 Four discharge models (A, B, C, and D) and seven discharge processes for LFP and NCM batteries are applied on LCA assessment.

Discharge model	A		B		C	D	
	ECR with Ferrocyanide		ECR without Ferrocyanide		Physical resistor	Chemical discharge	
Discharge process	A1	A2	B1	B2	C	D1	D2
Material	1 M Na ₂ SO ₄	1 M NaCl	1 M Na ₂ SO ₄	1 M NaCl	A 2 Ω of resistor	1 M Na ₂ SO ₄	1 M NaCl
	0.2 M K ₄ [Fe(CN) ₆]/K ₃ [Fe(CN) ₆]						

Tab. S4 Life cycle inventory of LFP batteries with different discharge processes
(processing one thousand LIBs).

	Type	Unit	A1	A2	B1	B2	C	D1	D2
Inupt	Water	kg			0.067	0.22		41.325	82.65
	Water	kg				1.295			4.835
	NaCl	kg						5.869	
	NaSO4	kg					1.534		
	Electricity	KWh	4.67	4.51	0.59	3.01			
Optput	Heat	g						0.008	0.216
	Li	g						0.25	0.4212
	Ni	g						0.1682	0.272
	Co	g						0.041	0.081
	Mn	g						0.125	0.269
	Fe	g						244	538
	COD	g						16.776	93.68
	TOC	g						0.238	0.348
	F	kg			0.067	0.22		41.325	82.65

Tab. S5 Life cycle inventory of NCM batteries with different discharge processes
(processing one thousand LIBs).

	Type	Unit	A1	A2	B1	B2	C	D1	D2
Inupt	Water	kg			0.415	0.434		41.325	165.3
	Water	kg				2.552			9.670
	NaCl	kg						5.870	
	NaSO4	kg					1.977		
	Electricity	KWh	10.084	9.992	3.661	5.940			
Optput	Heat	g						0.004	0.42
	Li	g						0.2088	0.5404
	Ni	g						0.166	0.276
	Co	g						0.035	0.181
	Mn	g						0.239	12.346
	Fe	g						270	706
	COD	g						17.188	254
	TOC	g						0.306	1.576
	F	kg			0.415	0.434		41.325	165.3

Tab. S6 Impact category of LCA and their Abbreviation.

Impact category	Abbreviation	Impact category	Abbreviation
Global warming potential	GWP	Marine ecotoxicity	METP
Ionizing radiation	IRP	Human carcinogenic toxicity	HTPc
Ozone formation, Human health	OFHH	Human non-carcinogenic toxicity	HTPen
Fine particulate matter formation	PMFP	Land use potential	LUP
Ozone formation, Terrestrial ecosystems	OFTE	Mineral resource scarcity	SOP
Terrestrial acidification	TAP	Fossil resource scarcity	FFP
Freshwater eutrophication	FEP	Water consumption	WCP
Marine eutrophication	MEP	Human health	HH
Terrestrial ecotoxicity	TEP	Ecosystems	ES
Freshwater ecotoxicity	FETP	Resources	RS

Tab. S7 List of background data considered in this study.

Type	Selected background data
Water	Tap water market for tap water Cut-off, U
Electricity	Electricity, medium voltage market group for electricity, medium voltage Cut-off, U
Na ₂ SO ₄	Sodium sulfate, anhydrite {RoW} market for sodium sulfate, anhydrite Cut-off, U
NaCl	Sodium chloride, powder {GLO} market for sodium chloride, powder Cut-off, U
Heat	Heat, district or industrial, other than natural gas {RoW} market for heat, district or industrial, other than natural gas Cut-off, U
Type	Selected background data
Water	Tap water {RoW} market for tap water Cut-off, U

Tab. S8 Table midpoint level environmental prices (€2015/unit).

Theme	Unit	Weighting factor
Climate change	€/kg CO ₂ -eq.	€ 0.06
Ozone depletion	€/kg CFC-eq.	€ 123
Human toxicity	€/kg 1,4 DB-eq.	€ 0.09
Photochemical oxidant formation	€/kg NMVOC-eq.	€ 1.15
Particulate matter formation	€/kg PM10-eq.	€ 39.20
Ionizing radiation	€/kg kBq U235-eq.	€ 0.05
Acidification	€/kg SO ₂ -eq.	€ 7.48
Freshwater eutrophication	€/kg P-eq.	€ 1.89
Marine eutrophication	€/kg N	€ 3.11
Terrestrial ecotoxicity	€/kg 1,4 DB-eq.	€ 8.69
Freshwater ecotoxicity	€/kg 1,4 DB-eq.	€ 0.04
Marine ecotoxicity	€/kg 1,4 DB-eq.	€ 0.01
Land use	€/m ² *year	€ 0.13

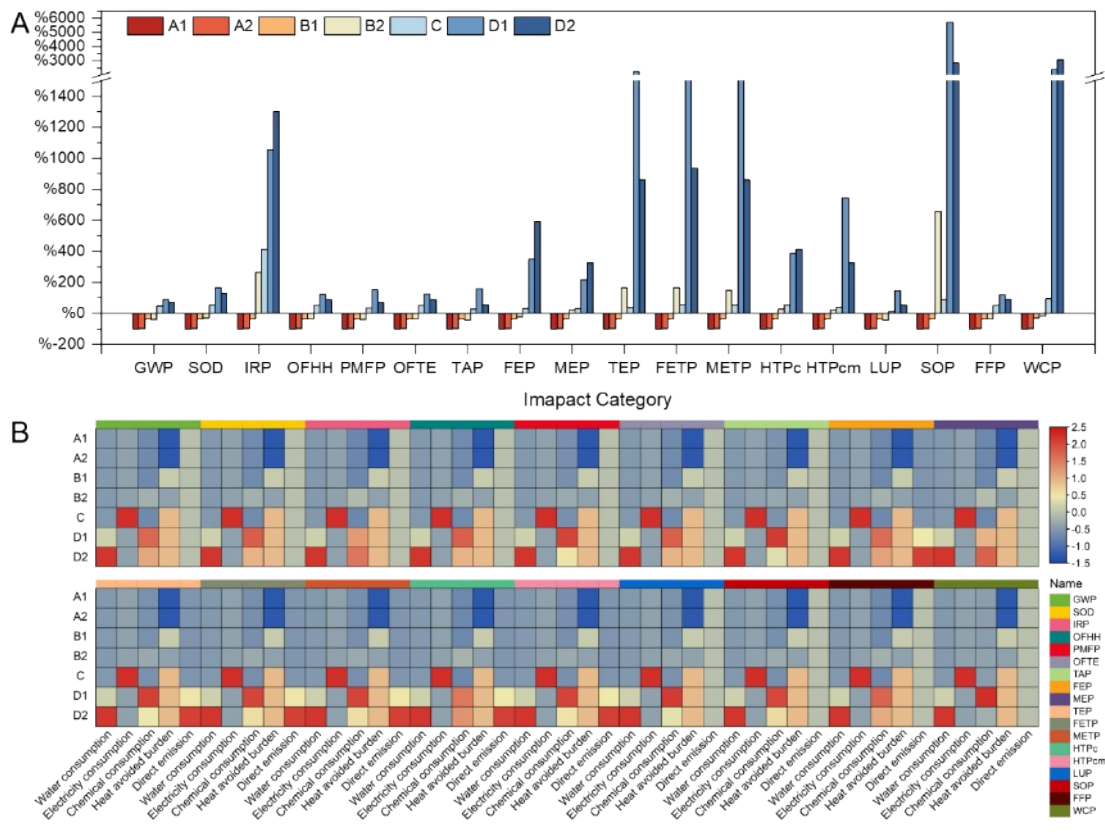


Fig. S18. LCA analysis of four discharge models (A, B, C, and D) for retired NCM LIBs (processing 1000 18650-type of LIBs). (A) The environmental impact assessment results of different discharge processes under three discharge models for NCM batteries. For all 18 impact categories, the A1 is defined as the reference for normalization. (B) Analysis of the contribution of discharge process to environmental impact under three discharge models for NCM batteries.

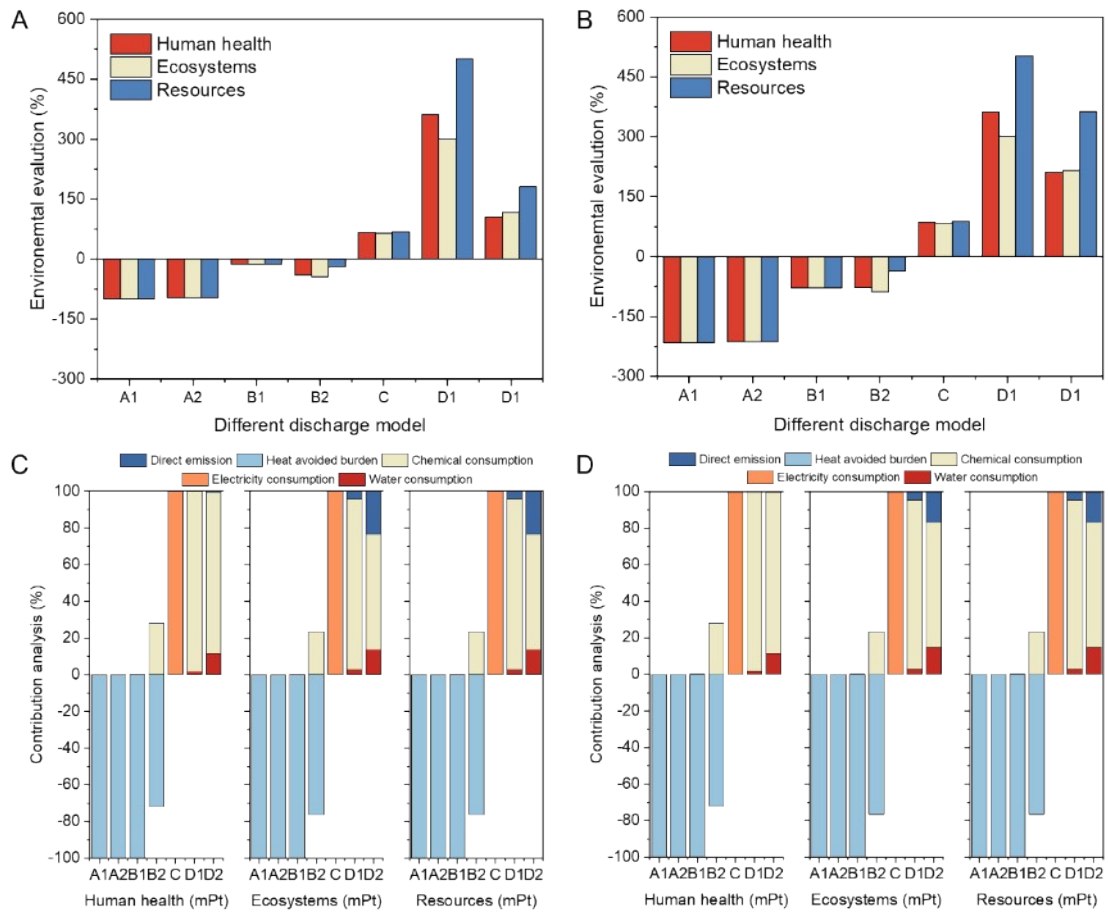


Fig. S19. End point environmental impact assessment results of four discharge models (A, B, C, and D, processing 1000 18650-type of LIBs). (A) LFP LIBs, for all 3 end point categories, the A1 is defined as the reference for normalization. (B) NCM LIBs, for all 3 end point categories, the A2 is defined as the reference for normalization. End point environmental impact contribution analysis of different discharge process. (C) LFP LIBs. (D) NCM LIBs.

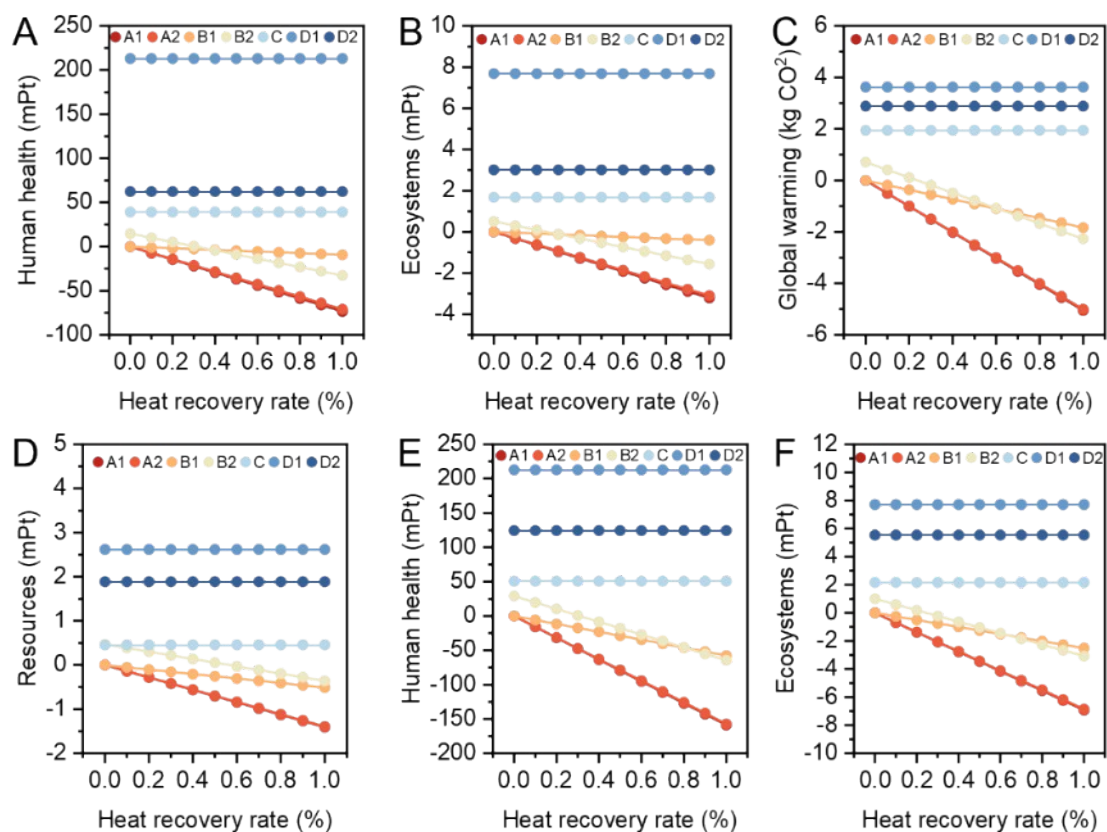


Fig. S20. The environmental impact of different heat energy recovery rate for four discharge models (A, B, C, and D, processing 1000 18650-type of LIBs). (A) Human health for LFP LIBs and **(B)** Ecosystems for LFP LIBs. **(C)** Global warming for NCM LIBs and **(D)** Resources for NCM LIBs. **(E)** Human health for NCM LIBs and **(F)** Ecosystems for NCM LIBs.

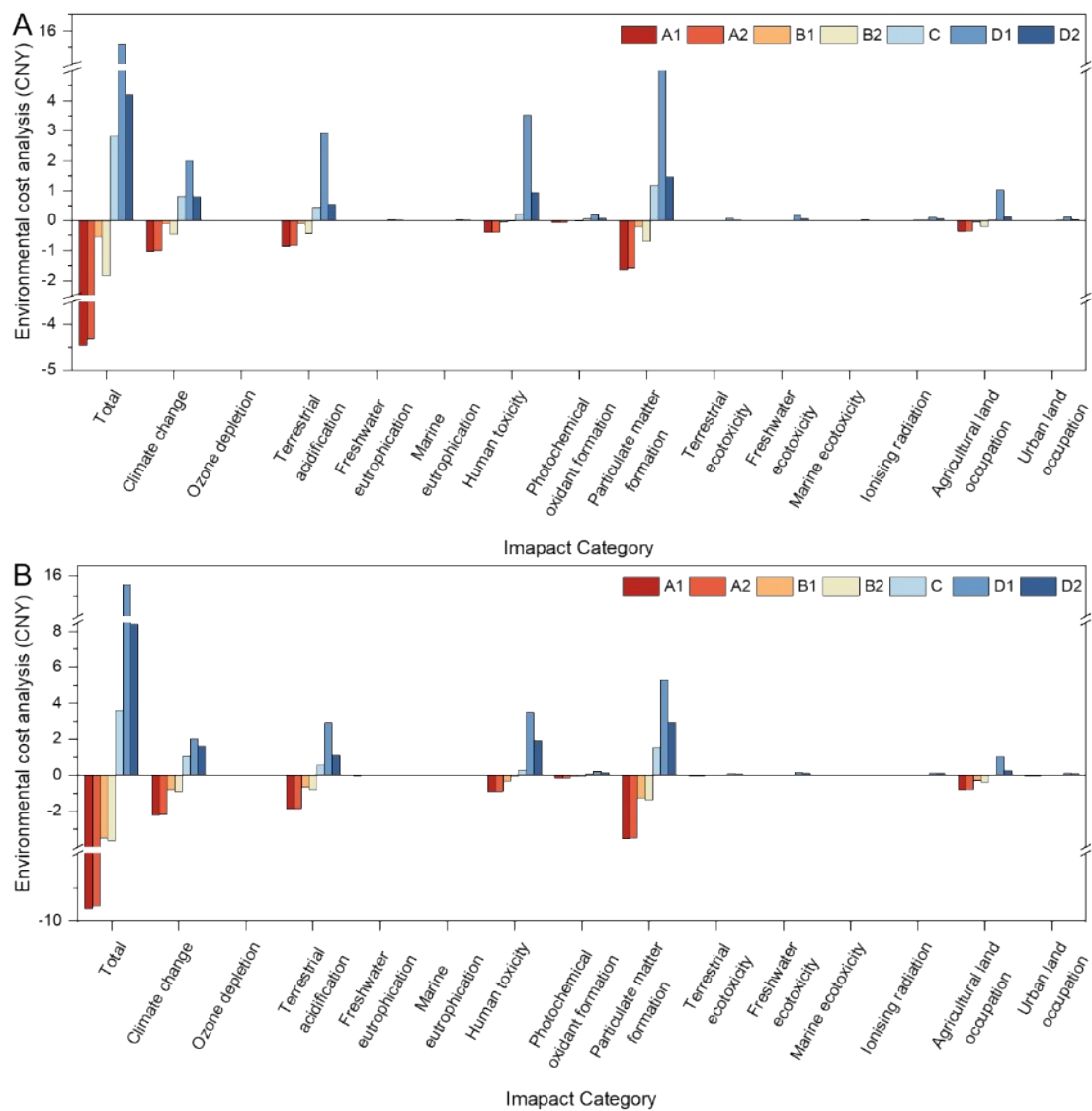


Fig. S21. Environmental cost analysis of four discharge models, which followed the Life cycle cost (LCC) analysis method. (A, B, C, and D, processing 1000 18650-type of LIBs). (A) LFP LIBs. (B) NCM LIBs.

References

- 1 Finkbeiner, M., Inaba, A., Tan, R., Christiansen, K. & Klüppel, H.-J. The new international standards for life cycle assessment: ISO 14040 and ISO 14044. *The international journal of life cycle assessment* 11, 80-85, (2006).
- 2 Huijbregts, M. A. et al. ReCiPe 2016: a harmonized life cycle impact assessment method at midpoint and endpoint level report I: characterization. (2016).
- 3 Wang, S. et al. Life cycle assessment and life cycle cost of sludge dewatering, conditioned with $\text{Fe}^{2+}/\text{H}_2\text{O}_2$, $\text{Fe}^{2+}/\text{Ca}(\text{ClO})_2$, $\text{Fe}^{2+}/\text{Na}_2\text{S}_2\text{O}_8$, and $\text{Fe}^{3+}/\text{CaO}$ based on pilot-scale study data. *ACS Sustain. Chem. Eng.* 11, 7798-7808, (2023).
- 4 Bijleveld, M. et al. Environmental prices handbook EU28 version. Methods and Numbers for Valuation of Environmental Impacts, (2018).